International Space Planes and Hypersonic Systems and Technologies Conferences
6-9 March 2017, Xiamen, China
21st AIAA International Space Planes and Hypersonics Technologies Conference

10.2514/6.2017-2155

Pressure and Heat Flux Calibration of the Long-test-duration Hypervelocity Detonation-driven Shock Tunnel

Qiu Wang[1], Ji-Wei Li[2], Pan Lu[3], Jin-Ping Li[4], Wei Zhao[5], and Zong-Lin Jiang[6]
State Key Laboratory of High Temperature Gas Dynamics, Institute of Mechanics, Chinese Academy of Sciences, Beijing, China, 100190

A large detonation-driven shock tunnel, named JF12, was developed for exploring hypersonic physics in Institute of Mechanics, Chinese Academy of Sciences. The shock tunnel is capable of duplicating the flight conditions and conducting full-scale or near full-scale model tests, which can make it easy for extrapolation of experimental data to flight. However, in view of the need for high-quality aerothermodynamic measurements in hypersonic shock tunnels, a detailed evaluation of the flowfield uniformity and standard model tests are necessary. In this paper, calibration of the Mach 8 nozzle was first presented. Pitot pressure and stagnation heat transfer data acquired using a Pitot rake were discussed to analyze the nozzle flow uniformity. Besides, a precision built 7-deg sharp cone instrumented with heat gages was used. Corresponding numerical simulations were also conducted for comparison. Results showed that good uniformity was found and a core flow region of approximately 1.8 to 2 m diameter was observed. And heat transfer measurement uncertainty was within ±10%, which was quite good in hypersonic shock tunnels currently.

Nomenclature

ρ	=	density, kg/m^3
c	=	heat capacity, J/(kg·K)
H	=	enthalpy, MJ/kg
k	=	thermal conductivity, enthalpy, J/(s·m^2·k)
Ms	=	Mach number of the incident shock wave in the shock tube
P	=	pressure, Pa
q	=	heat flux rate, MW/m^2
R	=	sphere radius, m
Re	=	freestream unit Reynolds number, 1/m
St	=	Stanton number
t	=	time, s
T	=	temperature, K
u	=	velocity, m/s
subscripts		
∞	=	freestream flow
0	=	stagnation parameters
1	=	parameters in the shock tube

[1] Assistant Professor, State Key Laboratory of High Temperature Gas Dynamics, No.15 Beisihuanxi Road, wangqiu@imech.ac.cn
[2] Student, State Key Laboratory of High Temperature Gas Dynamics, No.15 Beisihuanxi Road.
[3] Student, State Key Laboratory of High Temperature Gas Dynamics, No.15 Beisihuanxi Road.
[4] Associate Professor, State Key Laboratory of High Temperature Gas Dynamics, No.15 Beisihuanxi Road, lijinping@imech.ac.cn.
[5] Professor, State Key Laboratory of High Temperature Gas Dynamics, No.15 Beisihuanxi Road, zw@imech.ac.cn.
[6] Professor, State Key Laboratory of High Temperature Gas Dynamics, No.15 Beisihuanxi Road, Associate Fellow, zljiang@imech.ac.cn.

I. Introduction

Accurate prediction of physical or chemical effects influencing the aerodynamics at hypersonic velocities are critical to the design of hypersonic aerospace vehicles. Evaluation of the hypersonic phenomena on a particular vehicle design can be managed in one of three ways: flight test, simulation of flight condition in ground test facilities, or numerical simulations implementing models of physical and chemical processes, known as computational fluid dynamics (CFD). The first case is prohibitively expensive and reserved for the prototype design. CFD is a promising alternative with the advent of low cost, high power computing resources. However, it requires validation against with experimental data before confidently used. Unfortunately, high precision aerodynamic experimental data under hypersonic flows are limited, especially for the conditions where thermal chemical nonequilibrium prevails. Thus, ground test facilities, usually simulate partial relevant flow parameters, play an important role in the research of hypersonic flows, especially for simulating space vehicles' atmospheric reentry. And the development of experimental technique has made it possible to realize hypersonic flows range from 2.5 to 45 MJ/kg, which corresponds to velocities from 2 to 10 km/s, respectively [1, 2].Comprehensive overviews of ground based testing of hypersonic flows are given by Lu [3].

Among the hypersonic test facilities, shock tunnels show their advantages for the accommodation of relatively large-size models and low operational costs. In the view of enthalpy and pressure requirements, the shock tunnel must incorporate a high performance driver. Among the existing driving techniques, the detonation drivers are capable of producing high enthalpy and high pressure test flows simultaneously beside an easy operation and low capital investment [4]. In recent years, the backward and forward modes have been studied at LHD and crucial techniques, such as spontaneous strong ignition and attenuation of the reflected waves have also been resolved successively [5]. As a result of these improvements, a high enthalpy shock tunnel JF-10 was constructed in 1996. And followed by a large-scale shock tunnel JF12 in 2012, which is capable of reproducing the pure airflow with longer than 100 ms test duration. They could be useful tools for investigating into fundamental physics in hypersonic and high temperature gas flows [1, 6].

In this paper, the uniformity due to a free-stream of hypervelocity air expanded through a contoured nozzle was evaluated. A survey of the test flow was conducted by obtaining Pitot and heat flux rake measurements, or heat flux distribution on a 7 deg half-angle spherically sharp cone. Also the corresponding numerical simulations were carried out. Good uniformity was found and a core flow region of approximately 1.8 to 2 m diameter was observed, which could take the test of integrated vehicle/engine.

II. Experimental Facility and Apparatus

A. JF12 Shock Tunnel

The long-test-duration hypersonic detonation-driven shock tunnel was a reflected shock tunnel based on the backward detonation driver with several innovative techniques, as shown in Figure 1. And JF12 is named after shock tunnels under the serial number in LHD. It consists of a damping section, a detonation chamber, a shock tube, a nozzle and a test section. A heavy metal diaphragm separates the detonation chamber and the shock tube. The chamber is filled with a gaseous reactive mixtures, usually oxygen and hydrogen. Then strong incident shock waves in the shock tube can easily be generated by detonation product gases at high temperatures and pressures after simultaneously igniting the reactive mixtures. Moreover, JF12 is the largest shock tunnel in the world with the nozzle exit diameter of 2.5 m, capable of replicating flight conditions for Ma5~9 at altitude of 25~50 km and integrated vehicle/engine are possible to test. The major specifications of the shock tunnel is shown in Table1 and details can be seen in literature [5, 6].

Table 1 Facility parameters

Facility	JF12
Detonation chamber	99 m in length, 400 mm in diameter
Shock tube	89 m in length, 720 mm in diameter
Operation mode	backward mode
Nozzle	contoured 15 m in length, 2.5 m in exit diameter
Maximum H_0	5 MJ/kg

Figure 1 Photograph of JF12 long-test-duration detonation-driven shock tunnel

B. Rake Design Considerations

Figure 2 shows the rake probe configuration used in the experiments. The rake is 2.4 m long in both vertical and horizontal directions and 48 sensors could be installed along the rake in an equal interval at the same time. Pitot pressure and heat flux measurements were obtained to investigate the nozzle flow quality.

For the pitot pressure measurements, 24 NS-2 pressure transducers could be installed in vertical direction and 24 in the other direction. The pressure was measured between -1150 to 1150 mm at 100 mm intervals. Three different cross sections were validated here, 630 mm inside the nozzle, 1000 mm outside the nozzle and the nozzle exit.

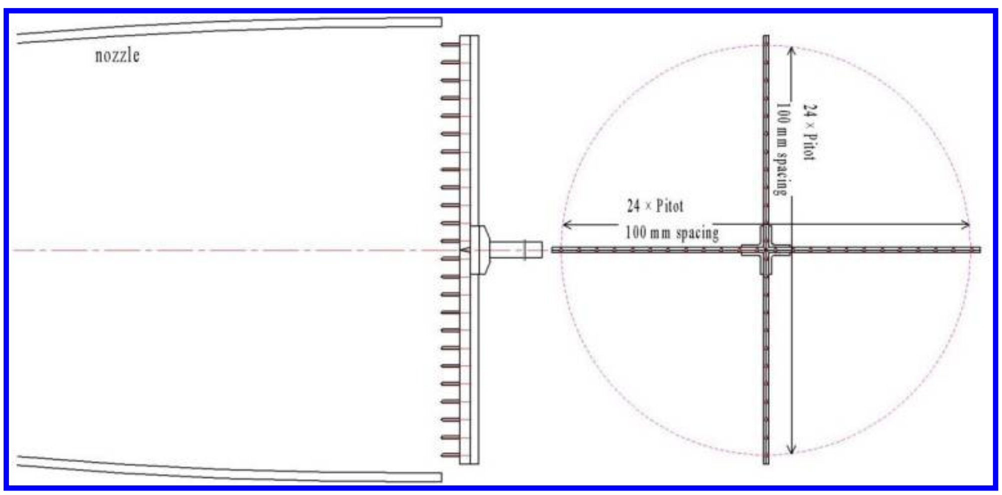

Figure 2 Rake probe configuration used for the flow survey experiments in JF12

For the heat flux measurements, a rake of 24 spheres of 30 mm in diameter was used. Using spheres was convenient as the theory can be used to provide a comparison with the experimental results. Home-made E-type (chromel-constantan) coaxial thermocouples which have fast response times and can be flush-mounted were installed to measure surface temperature. They were 1.4 mm in diameter. From the measured surface temperature T, the heat flux is calculated according to Schults and Jones [7] as follows:

$$\sqrt{\frac{\rho c k}{\pi}} \sum_{i=1}^{n} \frac{T(t_i)-T(t_{i-1})}{\sqrt{t_n - t_i} - \sqrt{t_n - t_{i-1}}} \qquad (1)$$

Where ρ, c and k are the density, heat capacity and heat conductivity of the sensor material, T and t are the temperature and time respectively. A typical temperature trace in the JF12 is shown in Figure 3.

Additionally, a 7 deg half-angle spherically sharp cone, with an overall length of 1100 mm, shown in Figure 4, was used to calibrate the flow-field. And calculating heat transfer had also been compared with the experiments.

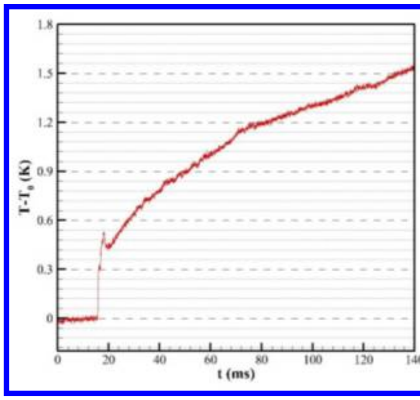

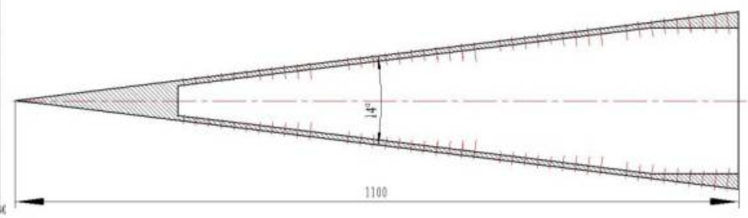

Figure 3 Typical temperature trace in JF12

Figure 4 Sharp cone model used in JF12

C. Calibration of the coaxial thermocouples

The coaxial thermocouples used in the JF12 shock tunnel, 1.4 mm in diameter, were newly developed these years in our institute. The effect of junction depth, thickness of the insulation between the two junction materials and influence of sensor installation on measuring accuracy has been considered. In addition, the thermocouples have also been calibrated in the shock tube, where the theory results could be obtained relatively accurately. Seven sensors were installed in a line at the stagnation point of a two dimension cylinder, with the radius to be 10 mm. The test conditions and heat flux results were shown in table 2, including the theory and experimental results. Free-stream parameters could be obtained using the shock tube theory and theory heat flux by the equation of Fay-Riddell. For the sensors in the seven runs, the max standard deviation was 8.4%. And the standard deviation between different sensors was 5%. Moreover, the maximum difference between the theory and experimental was 7%. The developed thermocouple can provide reliable support for heat transfer measurements in hypersonic shock tunnels.

Table 2 Facility parameters

Run No.	1	2	3	4	5	6	7	
T_1 [K]	24	24	24	24	24	23	23	
P_1 [kPa]	2.5	2.5	2.5	2.5	2.5	2.5	2.5	
M_S	2.98	2.98	2.98	2.98	2.97	2.98	2.97	
Theory Heat flux [MW/m^2]	1.51	1.51	1.51	1.51	1.49	1.51	1.49	average
Sensor 1	1.62	1.56	1.65	1.48	1.46	1.43	1.49	1.53
Sensor 2	1.48	1.51	1.53	1.39	1.39	1.53	1.44	1.47
Sensor 3	1.65	1.67	1.66	1.65	1.53	1.61	1.43	1.6
Sensor 4	1.54	1.54	1.50	1.42	1.52	1.58	1.54	1.52
Sensor 5	1.60	1.50	1.58	1.53	1.38	1.41	1.42	1.49
Sensor 6	1.39	1.43	1.46	1.50	1.39	1.65	1.42	1.46
Sensor 7	1.61	1.65	1.65	1.67	1.48	1.46	1.56	1.58

D. Numerical Simulations

As a valuable complement for the analysis of experimental results, numerical simulations were used in the paper. The governing equations employed were the axisymmetric, compressible Navier-Stokes equations. Calorically perfect gas was considered. The governing equations were solved using a finite difference approach; convective terms were approximated using the AUSMPW+ [8-9] scheme and central difference method was applied to the viscous terms. Time integration was performed implicitly by applying the LU-SGS algorithm [10]. No-slip and isothermal boundary conditions were specified as the boundary conditions at the wall, and temperature was set to 290K.

III. Results and Discussion

(1) Test Conditions

The reservoir and freestream conditions in our tests were shown in table 3. Reservoir pressure was measured using a piezoelectric pressure transducers mounted on the end of the shock tube. The conditions after the incident and reflected shocks were computed by using the initial state, the shock speed, and the equilibrium properties of the gas with Gaseq [11]. Unless the shock tube is perfectly tailored, the condition behind the reflected shock was different between the calculated pressure and the measured one. Then, reservoir state was computed assuming an isentropic process actually, from the calculated to the measured one. Based on the reservoir conditions, the freestream was subsequently determined by numerical re-building of nozzle flow.

Table 3 Test conditions

Condition		I	II
Reservoir	P_0 (MPa)	2.58	2.2
	H_0 (MJ/kg)	4.52	3.3
Freestream	T_∞ (K)	336	293
	u_∞ (m/s)	2771	2343
	p_∞ (Pa)	218	417
	Re/L (/m)	3.1×10^5	6.5×10^5

(2) Rake Probe Results

The rake calibration test was conducted at a stagnation enthalpy of 4.52 MJ/kg and a stagnations pressure of 2.58MPa, with other parameters shown in table 3. Figure 5 presented the stagnation and pitot pressure histories in one shot. The two agreed well for the steady test duration time, more than 100 ms.

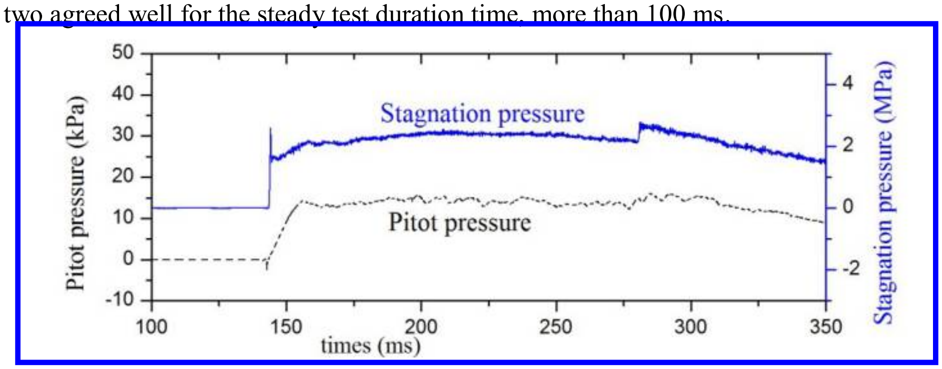

Figure 5 Stagnation and pitot pressure histories

Pitot pressure measurements obtained with the rake probe at three different cross sections were shown in Figure 6. The distributions indicated that a core flow approximately 1800 mm in diameter was produced by the Mach 8 nozzle at current conditions. Certainly, the core flow diameter would be larger under higher stagnation pressure conditions, with larger Reynolds numbers and thinner boundary layers. Even so, the effective test area was the biggest in similar facilities until now. However, the downside of the nozzle flow is its slight pressure drops due to the nozzle expansion.

The uniformity of heat flux variation across the nozzle exit plane was also investigated, with the results shown in Figure 7. The measurements were compared with the theory correlation by Filippis [12] as follows:

¿ $$10^{-5}\sqrt{\frac{P_t}{R_n}}H_0^{1.17} \tag{1}$$

where P_t was the pitot pressure measured, H_0 the freestream total enthalpy, and R_n the curvature radius, that was 15 mm. Table 4 presented the average heat flux, the standard deviation, and the difference between the average and the predicted value. The gauges in the boundary layer were not included. Overall, good uniformity was found in the core flow as the standard deviation was 7.8%. The measured average heat flux was slightly greater than the theory by 6%. However, the deviation was within the uncertainty of heat transfer measurements (±10%). We can say that reasonable agreement was obtained.

Table 4 Heat flux results

Heat flux (MW/m^2)	SD %	Theory (MW/m^2)	Δ %	CFD (MW/m^2)	Δ %
1.68	7.8	1.58	6	1.55	7.7

Heat transfer data obtained at hypersonic flows can also play an important role in code validation. In return, CFD readily provides detailed flow field information. Comparison between experimental data and CFD of the sphere pitot pressure and heat flux were also conducted. Considering the axial symmetry of the computing model, half of the geometries had been calculated in present study. The mesh size of 220×280 was applied, with 220 grid nodes across the axial coordinates. The grid spacing close to the wall in the stream-wise direction was 0.6×10^{-6} m. The calculated pressure and heat flux on the sphere wall was shown in figure 8. And the stagnation point pressure and heat flux at the nozzle exit were 16.1 kPa and 2.55 MW/m^2, respectively, where the average experimental values were 15.0 kPa and 1.68 MW/m^2. There was a difference of 7.3% and 7.7% for the two. Reasonable agreement is found between numerical simulations and experiment.

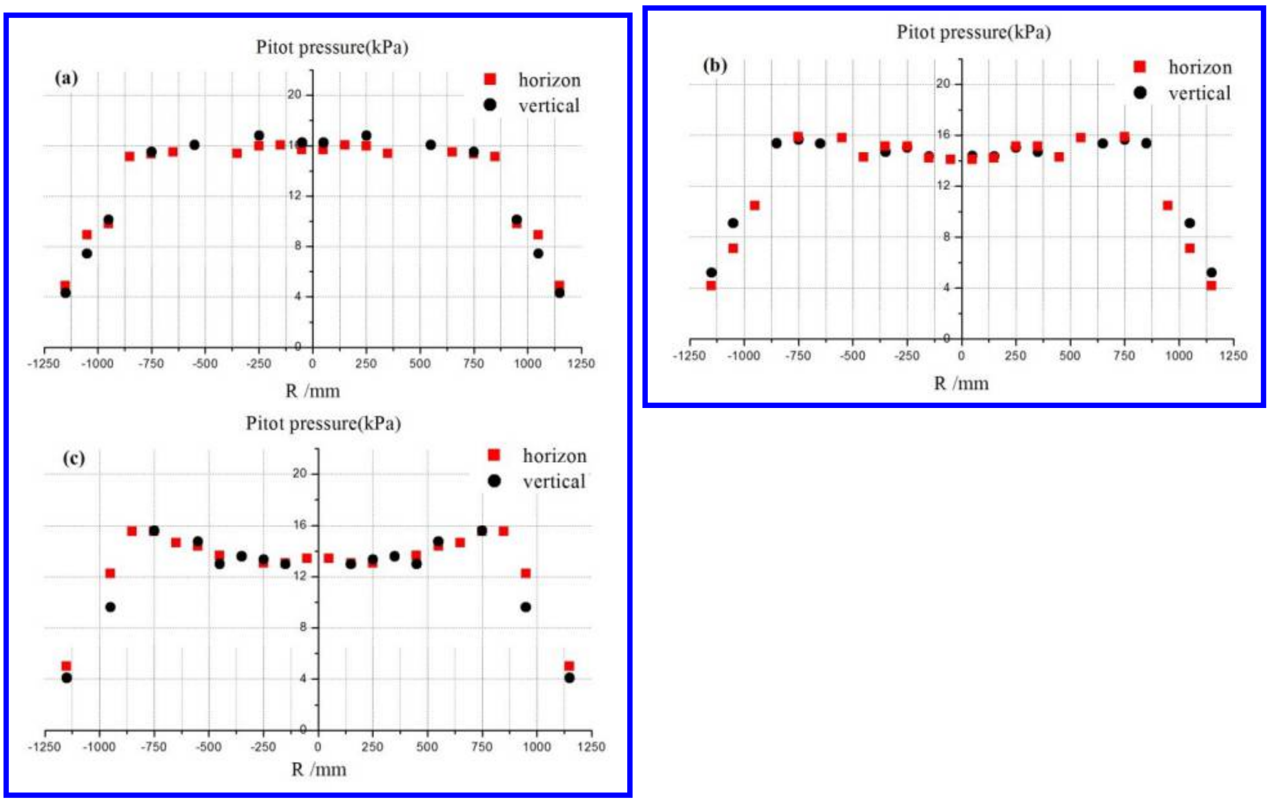

Figure 6 Pitot pressure distributions for Mach 8 nozzle at the conditions Ⅰ. (a) cross section 680 mm inside, (b) nozzle exit cross section, (c) cross section 1000 mm outside

(3) Sphere Cone Results

Stanton number (St) about experiment and theory along the surface of JF-12 model under condition Ⅱ was shown in Figure 4, where *St* is defined in equation (3),

$$St = \frac{q_w}{\rho_\infty u_\infty H_0} \qquad \mathrm{Re}_x = \frac{\rho_\infty u_\infty x}{\mu_\infty} \tag{3}$$

Equation (3) was usually used in aerodynamic experiments for what freestream parameters were known in general. x was the distance along the model to the tip. Gas condition for JF-12 was perfect gas and heat transfer on a sharp cone can be obtained by solving boundary layer equations easily [13]. The square, up-triangle and down-triangle in Figure 9 depicted heat flux distribution on the side, leeward and windward of the model, which showed good

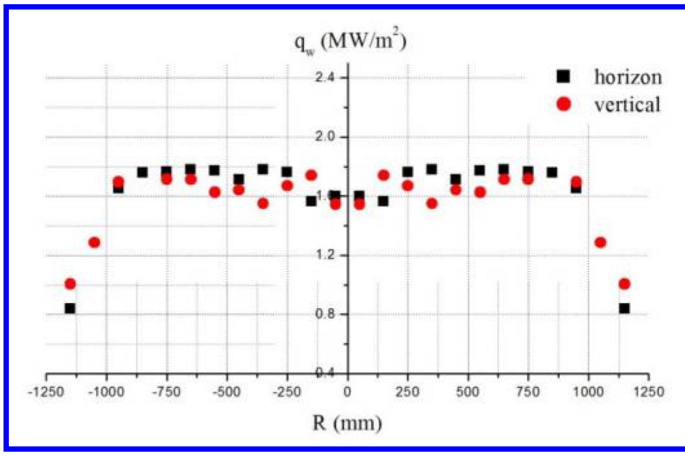

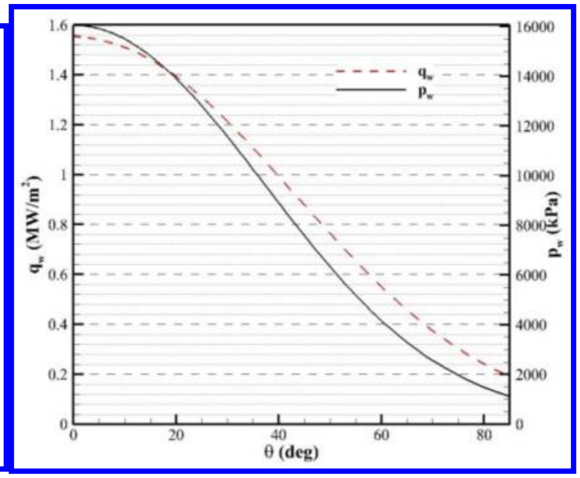

Figure 7 Heat flux distribution for Mach 8 nozzle at the condition Ⅰ, nozzle exit

Figure 8 Sphere wall heat flux and pressure distribution at the condition Ⅰ, nozzle exit

repeatability. It also revealed the good uniformity of the freestream flows. Comparison between Exp and theory showed that the experiment was within ±10% dispersion of the theoretical value, which was mainly come from the individual differences in thermocouple output voltages due to uneven quality. However, it was quite good for heat transfer measurements in hypersonic flows. Heat transfer data obtained at hypersonic flows can also play an important role in code validation. In return, CFD can easily give the flow field information in detail. Comparison between experimental data and CFD was shown in Figure 10. CFD results were slightly smaller than the experimental data. However, the deviation was within the uncertainty of heat transfer measurements (±10%). We can say that reasonable agreement between experiment and CFD was obtained. And it needed to be emphasized that the cell Reynolds number or grid independence were taken into account in our computation, which were not discussed in detail in the paper.

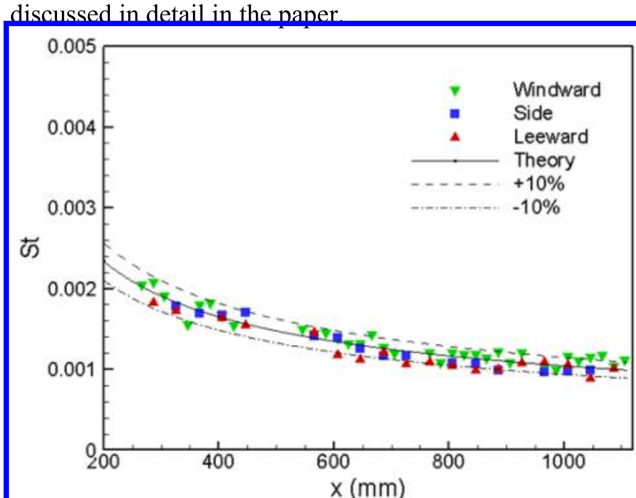

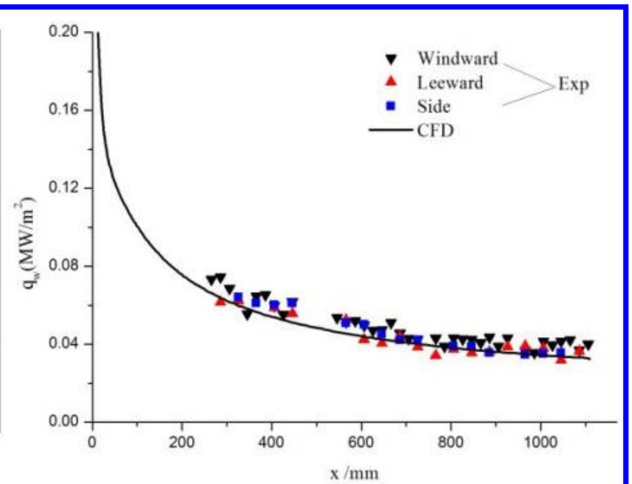

Figure 9 Heat transfer data comparison between Exp and theory [14]

Figure 10 Heat transfer data comparison between Exp and CFD in JF-12

IV. Conclusion

A large detonation-driven shock tunnel, named JF12, and home-made coaxial thermocouples were developed for exploring hypersonic physics in Institute of Mechanics, Chinese Academy of Sciences. Pitot pressure and stagnation heat transfer data acquired using a Pitot rake were discussed to analyze the nozzle flow uniformity. And a 7-deg sharp cone instrumented with heat gages was tested with corresponding numerical simulations. Results showed that good uniformity was found and a core flow region of approximately 1.8 to 2 m diameter was observed. And heat transfer measurement uncertainty was within ±10%, which was quite good in hypersonic shock tunnels currently.

Acknowledgments

The authors would like to thank Hong Chen, Chaokai Yuan and Shizhong Zhang for their cooperation. This work was supported by the National Natural Science Foundation of China (Grant Nos. 11402275, 11472280 and 11532014).

References

[1]Gai, S. L., and Nudford, N. R., "Stagnation Point Heat Flux in Hypersonic High Enthalpy Flows," *Shock Waves*, Vol. 2, No. 1, 1992, pp. 43-47.

[2]Kishimoto, T., Hanamitsu, A., and Bitoh, H., "High Enthalpy Flow Computation and Experiment Around the Simple Bodies," Tokyo: Special Publication of National Aerospace Laboratory SP-29, 1996, pp99-107.

[3]Lu, F. K., and Marren, D. E., *Advanced Hypersonic Test Facilities*, Progress in Astronautics and Aeronautics, 2002, pp. 198.

[4]Yu, H. R., Chen, H., and Zhao, W., "Advances in Detonation Driving Techniques for a Shock Tube/tunnel," *Shock Waves*, Vol. 15, No. 6, 2006, pp. 399-405.

[5]Zhao, W., Jiang, Z. L., Saito, T., Lin, J. M., Yu, H. R., and Takayama, K., "Performance of a Detonation Driven Shock Tunnel," *Shock Waves*, Vol. 14, No. 1-2, 2004, pp. 53-59.

[6]Jiang, Z. L., and Yu, H. R., "Experiments and Development of the Long-test-duration Hypervelocity Detonation-driven Shock Tunnel (LHDst)," *52nd Aerospace Sciences Meeting*, AIAA, Maryland, 2014-1012

[7]Schultz, D. L., and Jones, T. V., "Heat Transfer Measurements in Short Duration Facilities," AGARD-AG-165, 1973.

[8]Kim, K. H., Kim, C., and Rho O. H., "Methods for the Accurate Computations of Hypersonic Flows: I. AUSMPW+ Scheme," *Journal of Computational Physics*, Vol. 174, No. 1, 2001, pp. 38-80.

[9]Kitamura, K., Shima, E., Nakamura, Y., and Roe, P., "Evaluation of Euler Flux for Hypersonic Heating Computations," *AIAA Journal*, Vol. 48, No. 4, 2010, pp. 763-776.

[10]Jameson, A., and Yoon, S., "Lower-Upper Implicit Schemes with Multiple Grids for the Euler Equations," *AIAA Journal*, Vol. 25, No. 7, 1987, pp. 929-935.

[11]Morley, C., Gaseq, Ver. 0.79, URL: http://www.gaseq.co.uk/, 2005.

[12]Filippis, F. D., Savino, R., and Martucci, A., "Numerical-experimental Correlation of Stagnation Point Heat Flux in High Enthalpy Hypersonic Wind Tunnel," *AIAA/CIRA 13th International Space Planes and Hypersonics Systems and Technologies Conference,* AIAA, Capua, Italy, 2005-3277.

[13]Anderson, J. D., *Hypersonic and High Temperature Gas Dynamics*, McGraw-Hill Book Company, New York, 1989.

[14]Wang, Q., Li, J. P., Zhao, W., Jiang, Z. L., "*Comparative Study on Aerodynamic Heating under Perfect and Nonequilibrium Hypersonic Flows*," *Science China Physics Mechanics and Astronomy*, Vol. 59, No. 2: 624701, 2016.